Synthetic curcuminoids modulate the arachidonic acid metabolism of human platelet 12-lipoxygenase and reduce sprout formation of human endothelial cells

Jerzy Jankun,[1,2] Ansari M. Aleem,[1] Sylvia Malgorzewicz,[1] Maria Szkudlarek,[1] Maria I. Zavodszky,[3] David L. DeWitt,[3] Michael Feig,[3] Steven H. Selman,[1,2] and Ewa Skrzypczak-Jankun[1]

[1]Urology Research Center, Department of Urology; [2]Physiology and Molecular Medicine, Medical University of Ohio, Toledo, Ohio; and [3]Department of Biochemistry and Molecular Biology, Michigan State University, East Lansing, Michigan

Abstract

Platelet 12-lipoxygenase (P-12-LOX) is overexpressed in different types of cancers, including prostate cancer, and the level of expression is correlated with the grade of this cancer. Arachidonic acid is metabolized by 12-LOX to 12(*S*)-hydroxyeicosatetraenoic acid [12(*S*)-HETE], and this biologically active metabolite is involved in prostate cancer progression by modulating cell proliferation in multiple cancer-related pathways inducing angiogenesis and metastasis. Thus, inhibition of P-12-LOX can reduce these two processes. Several lipoxygenase inhibitors are known, including plant and mammalian lipoxygenases, but only a few of them are known inhibitors of P-12-LOX. Curcumin is one of these lipoxygenase inhibitors. Using a homology model of the three-dimensional structure of human P-12-LOX, we did computational docking of synthetic curcuminoids (curcumin derivatives) to identify inhibitors superior to curcumin. Docking of the known inhibitors curcumin and NDGA to P-12-LOX was used to optimize the docking protocol for the system in study. Over 75% of the compounds of interest were successfully docked into the active site of P-12-LOX, many of them sharing similar binding modes. Curcuminoids that did not dock into the active site did not inhibit P-12-LOX. From a set of the curcuminoids that were successfully docked and selected for testing, two were found to inhibit human lipoxygenase better than curcumin. False-positive curcuminoids showed high LogP (theoretical) values, indicating poor water solubility, a possible reason for lack of inhibitory activity or/and nonrealistic binding. Additionally, the curcuminoids inhibiting P-12-LOX were tested for their ability to reduce sprout formation of endothelial cells (*in vitro* model of angiogenesis). We found that only curcuminoids inhibiting human P-12-LOX and the known inhibitor NDGA reduced sprout formation. Only limited inhibition of sprout formation at ~IC_{50} concentrations has been seen. At IC_{50}, a substantial amount of 12-HETE can be produced by lipoxygenase, providing a stimulus for angiogenic sprouting of endothelial cells. Increasing the concentration of lipoxygenase inhibitors above IC_{50}, thus decreasing the concentration of 12(*S*)-HETE produced, greatly reduced sprout formation for all inhibitors tested. This universal event for all tested lipoxygenase inhibitors suggests that the inhibition of sprout formation was most likely due to the inhibition of human P-12-LOX but not other cancer-related pathways. [Mol Cancer Ther 2006;5(5):1371–82]

Introduction

Several studies have implicated the role of dietary fatty acids, especially arachidonic acid, in prostate cancer formation and progression (1, 2). Three types of enzymes [cyclooxygenases, epoxygenases (cytochrome *P*450), and lipoxygenases] can metabolize this acid. Most cancer-related research has been done on cytochromes and cyclooxygenases, but much less is known about lipoxygenases. Human lipoxygenases (~670 amino acids) are divided into several major categories [5-lipoxygenase (5-LOX), 8-LOX, 11-LOX, 12-LOX, and 15-LOX] depending on the outcome of arachidonic acid peroxidation (3). A growing body of evidence points to the crucial role of 12-LOX involvement in prostate cancer.

Originally, platelet-type 12-LOX (P-12-LOX) was believed to be expressed solely in platelets, HEL cells, and umbilical vein endothelial cells (4). However, P-12-LOX expression has been detected in various cell lines (DU-145, LnCAP, and PC-3) and tumor tissues, including the prostate (5). Gao et al. (6) found that P-12-LOX mRNA expression was significantly higher in prostate adenocarcinoma tissue compared with matched normal prostate epithelium, and that this increased expression is correlated with advanced stage and grade of adenocarcinomas. In their study, tissues from >130 patients were examined with 38% showing elevated P-12-LOX mRNA in malignant tissue compared with normal matched tissue. The level of elevation of P-12-LOX expression among

Received 1/13/06; revised 2/20/06; accepted 3/17/06.

Grant support: NIH grants CA90524 and CA109625 and Frank D. Stranahan Endowment Fund for Oncological Research.

The costs of publication of this article were defrayed in part by the payment of page charges. This article must therefore be hereby marked advertisement in accordance with 18 U.S.C. Section 1734 solely to indicate this fact.

Note: The present address for S. Malgorzewicz is Department of Clinical Nutrition, Institute of Internal Medicine, Medical University of Gdansk, 80-211 Gdansk, Poland.

Requests for reprints: Jerzy Jankun, Urology Research Center, Medical University of Ohio, 3065 Arlington, Toledo, OH 43614-5807. Phone: 419-383-3691; Fax: 419-383-3785. E-mail: jerzy@meduohio.edu, http://golemxiv.dh.mco.edu/~jerzy/

Copyright © 2006 American Association for Cancer Research.

doi:10.1158/1535-7163.MCT-06-0021

high-grade prostatic adenocarcinomas compared with that of low- and intermediate-grade prostatic adenocarcinoma proved statistically significant. Some studies suggest an association among prostate cancer progression, metastasis, and an elevated expression of P-12-LOX (6, 7). Furthermore, it was suggested that prostate cancer cells express several megakaryocytic genes (*adhesion receptors α IIb, β3, thrombin receptor*, and *PECAM/CD31* and/or *P-12-LOX*) mimicking platelet cells, which help in cancer hematogenous dissemination (8).

Arachidonic acid is metabolized by 12-LOX to 12(*S*)-hydroxyeicosatetraenoic acid [12(*S*)-HETE], and this biologically active metabolite has been reported to be potentially involved in prostate cancer development by modulating cell proliferation (1, 9, 10). 12(*S*)-HETE has also been shown to play a significant role in the processes of tumor-induced angiogenesis and metastasis. 12(*S*)-HETE possesses mitogenic properties for microvascular endothelial cells (11) and can promote endothelial cell migration (12). Surface expression of integrin $\alpha_v\beta_3$, a tumor-induced angiogenic vasculature–related endothelial cell integrin, is up-regulated by 12(*S*)-HETE, promoting integrin translocation from intracellular pools (13). Furthermore, 12(*S*)-HETE can induce endothelial cell cytoskeletal rearrangement, resulting in endothelial cell retraction (14), a necessary step for tumor cell extravasations. In addition, 12(*S*)-HETE can stimulate tumor cell motility (15) and augment the invasive potential of AT2.1 rat prostate tumor cells (16). Through a protein kinase C–dependent pathway, 12-HETE has been reported to modulate the release of the lysosomal enzyme cathepsin B in MCF10AneoT human mammary carcinoma cells and murine B16a melanoma cells (10). Our own studies show that P-12-LOX overexpression in human prostate cancer (PC3) cells promotes the increased accumulation of 12(*S*)-HETE and vascular endothelial growth factor in culture media, leading to constitutive extracellular signal-regulated kinase 1/2 phosphorylation. This process is driven by 12(*S*)-HETE that stimulate extracellular signal-regulated kinase 1/2 phosphorylation via a pertussis toxin–sensitive G-protein–coupled receptor and mitogen-activated protein/extracellular signal regulated kinase kinase (17).

Recent studies have verified the significant role that 12(*S*)-HETE plays in tumor related angiogenesis. Nie et al. (12) used nude mice injected with human prostate PC-3 cancer cells overexpressing P-12-LOX to show that P-12-LOX-transfected cells grow faster *in vivo* and form larger tumors, and that there was a positive correlation between tumor size and increased tumor angiogenesis. In a similar study, Connolly and Rose (18) injected P-12-LOX overexpressing human breast MCF-7 cancer cells into nude mice and showed that P-12-LOX could accelerate the growth rate and the tumor volume due to increased angiogenic-stimulating properties. Furthermore, Pidgeon et al. (1) showed that treatment of PC-3 and DU145 human prostatic cancer cells with P-12-LOX inhibitors baicalein and *N*-benzyl-*N*-hydroxy-5-phenylpentamine resulted in significant apoptosis of these prostate cancer cells. In addition, PC-3 cells showed a decrease in phosphorylated retinoblastoma protein and inhibition of other retinoblastoma-associated proteins (p107 and p130). Of significance in this study was that treatment with baicalein blocked the loss of phosphorylated retinoblastoma protein; however, the addition of 12(*S*)-HETE induced phosphorylated retinoblastoma protein expression. In addition, the addition of 12(*S*)-HETE reversed baicalein-induced apoptosis, whereas other lipoxygenase metabolites, 5(*S*)-HETE, or 15(*S*)-HETE did not. The authors suggest that these results stress the critical role of the 12-LOX pathway in the regulation of prostate cancer progression and apoptosis. They also strongly endorse the idea that inhibitors of 12-LOX are potential therapeutic agents in the treatment of prostate cancer (1). We have found that baicalein reduces sprout formation and tumor size of human prostate xenografts (PC3 and DU145) in experimental animals (19).

India is the one of the countries with the most diverse populations and diets in the world. Rates for colorectal, prostate, and lung cancers in that country (despite population and diet diversity) are one of the lowest in the world. Of particular interest for cancer prevention in India is the role of turmeric (curcumin), one of the most common Indian spices (20). Curcumin is also used in Indian traditional medicine for various ailments and through different routes of administration, including topical, oral, and by inhalation (21). This chemical is a naturally occurring polyphenolic phytochemical isolated from the powdered rhizome of the plant *Curcuma longa*. Curcumin has known anti-inflammatory properties and was used for generations in folk medicine for that purpose. Traditionally, two possible mechanisms of curcumin (diferuloyl methane) for protection against cancer have been postulated: (*a*) antioxidant property and (*b*) antioxidant-dependent induction of detoxifying enzymes (22). However, curcumin can down-regulate the expression and activity of some other enzymes important in cancerogenesis, including cyclooxygenases and lipoxygenases (23–25). Limiting factors in the therapeutic use of curcumin are its relatively low IC_{50} and bioavailability. By employing homology modeling to predict the structure of the human P-12-LOX and using this structure as target for docking, we were able to predict a possible binding mode of curcumin in the active site of human P-12-LOX that is identical to soybean lipoxygenase determined by X-ray experiment (26). Using the same target, we then screened a variety of curcumin derivatives in search of better and novel human lipoxygenase inhibitors.

Materials and Methods

Homology Modeling of P-12-LOX

The structure of P-12-LOX is unknown. However, a model has been created using an automated protein modeling server, Swiss Model (27, 28), which is based mainly on the homology to the known structure of rabbit lipoxygenase, PDB entry 1-LOX (29). Additional structures used in modeling included soybean lipoxygenases 2SBL (30), 1NO3 (31), 1JNQ (32), and 1IK3 (33) and human autocrine motility factor 1JIQ (34).

The model was visually examined, manually corrected to avoid unfavorable conformations and steric constrains, meet the commonly used validation criteria, and minimize potential energy using the programs CHAIN, (35), Modeller (36, 37), and CHARMM (38). Subsequently, short molecular dynamics simulations were done with CHARMM and the MMTSB Tool Set (39).

Docking of Small Organic Molecules to P-12-LOX Using SLIDE

SLIDE is a docking/screening tool using distance geometry techniques to match ligand interaction points to template points describing the binding site of the target protein (40). The template consists of points identified as the most favorable positions for ligand atoms to form hydrogen bonds or make hydrophobic interactions with the neighboring protein atoms (41). After the initial matching step, SLIDE uses full atom representation of both the ligand and the target protein to model induced fit upon binding and score the complex based on hydrophobic complementarity and the number of protein-ligand hydrogen bonds. Residues within 9.0 Å of the binding site cavity of P-12-LOX were used as the target for the docking.

Evaluation of Ligand-Protein Complex Formation

In addition to the built-in scoring function of SLIDE, DrugScore was used to score the dockings. Although SLIDE evaluates the predicted protein-ligand complex based on geometric and chemical complementarity, DrugScore will estimate the binding affinity based on the statistical preferences of ligand atoms to be found near various protein atoms observed in known crystal complexes (40–42). Both of these scoring functions were trained on experimental data and then tested on an independent set of diverse enzymes, with statistical analysis done to evaluate the correlation between predicted scores and experimentally measured binding affinities (42). Once they were validated this way, it is not necessary to perform statistical analysis for every system the scoring function is applied to. The ligand candidates were ranked based on their consensus score computed as the sum of their normalized DrugScores and SLIDE scores, and that was the most important single criteria used to select the best candidates to inhibit P-12-LOX. In addition, we have visually inspected the docked orientations to exclude docked ligand orientations with parts of the ligand exposed to the solvent and/or unoccupied cavities left in the binding site.

Molecular Graphics

SwissPDB, Chain v.7, and PyMOL viewers were used to display the three-dimensional structures of P-12-LOX and to generate POV-Ray scenes (43).

Expression and Purification of P-12-LOX

Human P-12-LOX with a 6-His tag on the NH_2 terminus inserted into the pFastBac1 vector (Life Technologies, Gaithersburg, MD) was a generous gift of Dr. Holman (University of California, Santa Cruz, CA; ref. 44). Expression and purification were done basically as described before (44). In pFastbac vector, the expression of the gene is controlled by the *Autographa californica* multiple nuclear polyhedrosis virus (AcMNPV) polyhedrin or p10 promoter for high-level expression in insect cells. The plasmids were then transposed into a recombinant bacmid with the help of DH10Bac *Escherichia coli* cells (Invitrogen, Carlsbad, CA), which contain a baculovirus shuttle vector (Bacmid) with a min-attTn7 target site and a helper plasmid. Transposition occurs between the mini-Tn7 element on the pFastBac vector and the mini-attn7 target site on the bacmid to generate a recombinant bacmid. This transposition reaction occurs in the presence of transposition proteins supplied by the helper plasmid. This high molecular weight recombinant bacmid DNA was isolated from the white colonies grown for 48 hours at 37°C on a Luria-Bertani agar plate containing 50 μg/mL kanamycin, 7 μg/mL gentamicin, 10 μg/mL tetyracycline, 100 μg/mL X-gal, and 40 μg/mL isopropyl-L-thio-B-D-galactopyranoside. Recombinant bacmid DNA was used to transfect Sf9 cells derived from *Spodoptera frugiperda* (Fall armyworm) using cellfectin reagent (Invitrogen) and following the instruction provided. The virus generated was P1 viral stock. The virus was subsequently amplified to $\sim 2 \times 10^7$ plaque forming units/mL. This virus was then added to Sf9 cells ($\sim 2 \times 10^6$/mL) at a concentration of $\sim 2 \times 10^7$ plaque forming units/mL in 6- or 24-well tissue culture plates. The plates were incubated at 27°C in a humidified chamber for different time intervals. The cells were harvested and lysed in 62.5 mmol/L Tris-HCl (pH 6.8), 2% SDS and analyzed by SDS-PAGE and Western blot using an anti-histidine tag antibody (no anti-P-12-LOX antibody is available).

Nonreducing Gel Electrophoresis

The electrophoresis was done at room temperature in gradient gels with 4% to 12% polyacrylamide, in the absence of 2-mercaptoethanol. Gels were stained with Colloidal Coomassie Blue (Invitrogen).

In-Gel Digestion with Trypsin

The protein band was excised from a 4% to 12% gradient SDS-PAGE gel and destained with 30% methanol for 3 hours at room temperature. In-gel proteolysis was done with sequencing grade trypsin (Promega, Madison, WI) and was carried out as described previously (45). Briefly, a gel slice was washed with 150 μL of 50% acetonitrile in 0.1 mol/L ammonium bicarbonate buffer (pH 8) for 30 minutes. The gel slice was then diced into small cubes and dried under vacuum. Trypsin (0.5 μg) was added in a minimal volume of 0.1 mol/L ammonium bicarbonate buffer, and digestion was carried out for 16 hours at 37°C with an additional aliquot of trypsin (0.25 μg) added after 12 hours. Peptides were extracted once with 150 μL of 60% acetonitrile, 0.1% trifluoroacetic acid for 30 minutes followed by a further extraction with 100 μL of the same solution. All extracts were pooled and concentrated using Vacufuge to a final volume of 10 μL.

Protein Identification by Peptide Sequencing Using Liquid Chromatography

Tandem mass spectrometry (liquid chromatography tandem mass spectrometry) was done at Proteomics Laboratory, Program in Bioinformatics and Proteomics/Genomics at the Medical University of Ohio (45). Two microliters of the digest were separated on a reverse-phase

column (Aquasil C18, 15 μm tip × 75 μm id × 5 cm Picofrit column; New Objectives, Woburn, MA) using acetonitrile/1% acetic acid gradient system (5–75% acetonitrile over 35 minutes followed by 95% acetonitrile wash for 5 minutes) at a flow rate of 250 nL/min. Peptides were directly introduced into an ion-trap mass spectrometer (LCQ, ThermoFinnigan) equipped with a nanospray source. The mass spectrometer was set for analyzing the positive ions and acquiring a full mass spectrometry scan and a collision-induced dissociation spectrum on the most abundant ion from the full mass spectrometry scan (relative collision energy ~30%). Dynamic exclusion was set to collect three collision-induced dissociation spectra on the most abundant ion and then exclude it after 2 minutes. Collision-induced dissociation spectra were manually verified by comparing against an *in silico* tryptic digest of P-12-LOX sequence using the MS-Digest and MS-Product provisions of Protein Prospector.[4]

Iron Content in P-12-LOX

The iron content was determined independently by two different methods. First, it was measured by atomic absorption spectroscopy (spectrometer Varian AA-1275). The second measurement was done by inductively coupled plasma optical emission spectroscopy (Shimadzu Trace TOC Analyzer at Galibraith Laboratories, Inc., Knoxville, TN).

Inhibitors of P-12-LOX

The curcuminoids were a generous gift from Dr. Richard Hart and were synthesized and purified as described before (46).

Determination of IC_{50}

The enzyme activity was determined as described before (44). The inhibitory activity of curcuminoids was determined by direct measurement of the 12(*S*)-HETE formation as measured by the increase of absorbance at 234 nm [25 mmol/L HEPES (pH 8), 3 μmol/L arachidonic acid]. The reaction was done in a buffer and 200 nmol/L of enzyme stirred with a rotating stir bar in the beginning of the assay (23°C). IC_{50} values were determined by measuring the enzymatic rate at a variety of inhibitor concentrations (depending on the inhibitor strength) and plotting their values versus inhibitor concentration. The corresponding data were fitted to a simple saturation curve, and the inhibitor concentration at 50% activity was determined (IC_{50}). The inhibitors were typically dissolved in DMSO or ethanol at a concentration of 1 mg/mL (44).

P-12-LOX pH Activity Dependence

Enzyme activity was done as described above in pH 7.0 to 8.0 (in 0.2 increments) and additionally at pH 8.5.

Sprout Formation Assay

Human umbilical vascular endothelial cells (HUVEC) were grown to confluence in an EGM-2 growth medium. Next, the cells were trypsinized and seeded onto 0.5% agarose-coated culture dishes. This procedure resulted in cell aggregate formation after 24 hours of incubation at 37°C. HUVEC aggregates were decanted by allowing the cells to stand for 30 minutes at room temperature. The old medium supernatant was decanted, and HUVEC aggregates were suspended in 5 mL of fresh EGM-2 growth medium. Three-dimensional fibrin gels were prepared by mixing the following in 12-well culture plates: 960 μL of human fibrinogen (type III, 60% of protein clotable; 2.50 mg/mL concentration in RPMI 1640), 40 μL of HUVEC aggregate suspension, and 12.5 μL of human thrombin (25 IU/mL concentration in RPMI 1640). The mixture was gently mixed and allowed to gel for about 4 minutes at 37°C before adding EGM-2 growth medium over the gel.

The sprout formation assay was done as described by Pepper et al. (47). Briefly, HUVEC aggregates were suspended in fibrin gel containing P-12-LOX inhibitors; 1 mL of EGM-2 growth medium was later added over the fibrin gel. After 3 days of cell incubation, cultures were fixed *in situ* for 24 hours with 2 mL of 10% formalin solution and photographed under a phase-contrast microscope. Measurements were carried out in duplicate for three to six independent HUVEC aggregates.

Statistical Analysis

The Kruskal-Wallis test was done for normality with multiple comparisons between all groups (Mann-Whitney test). The differences were considered significant for $P < 0.05$ (11.5.1 SPSS for Windows).

Results and Discussion

Modeling of the Human P-12-LOX Molecular Structure

Although ~50 sequences of different lipoxygenases have been determined for plant and mammalian enzymes, structural data are available for only three enzymes: soybean LOX-1 and LOX-3 and rabbit 15-LOX. Despite the differences in size (LOX-3, 857 residues; rabbit 15-LOX, 663 residues; human P-12-LOX, 662 residues), these proteins have a 62% homology, and plant and rabbit enzymes show the same topology. In addition, the rabbit reticulocyte 15-LOX exhibits the best overall alignment to the human gene sequence with BLAST (48). The only known structure of the mammalian enzyme lacks structural information about the crucial fragments near the active site (see broken ends pointed to by the magenta arrows in Fig. 1A). An automatic routine cannot provide reliable model for the missing part, and it was obvious that upper fragment, depicting a stretched coil and a pin-like structure (Fig. 1B, *red*), was unrealistic because predictions based on sequence call for the formation of the helical structure there. In addition, such model can and often does contain steric constraints and bumps in the whole model. Therefore, this theoretical model was carefully examined; the main chain and side chains were corrected to avoid collisions and improve the torsion angles to better fit the common acceptance criteria and possible hydrogen bonding network; and the model was validated using PDB validation tools (Fig. 1B, *light green*). Independently, the fragments missing in rabbit lipoxygenase and those of a questionable quality in the theoretical model were examined by performing short, restrained molecular dynamics simulations, resulting in two alternate

[4] http://prospector.ucsf.edu

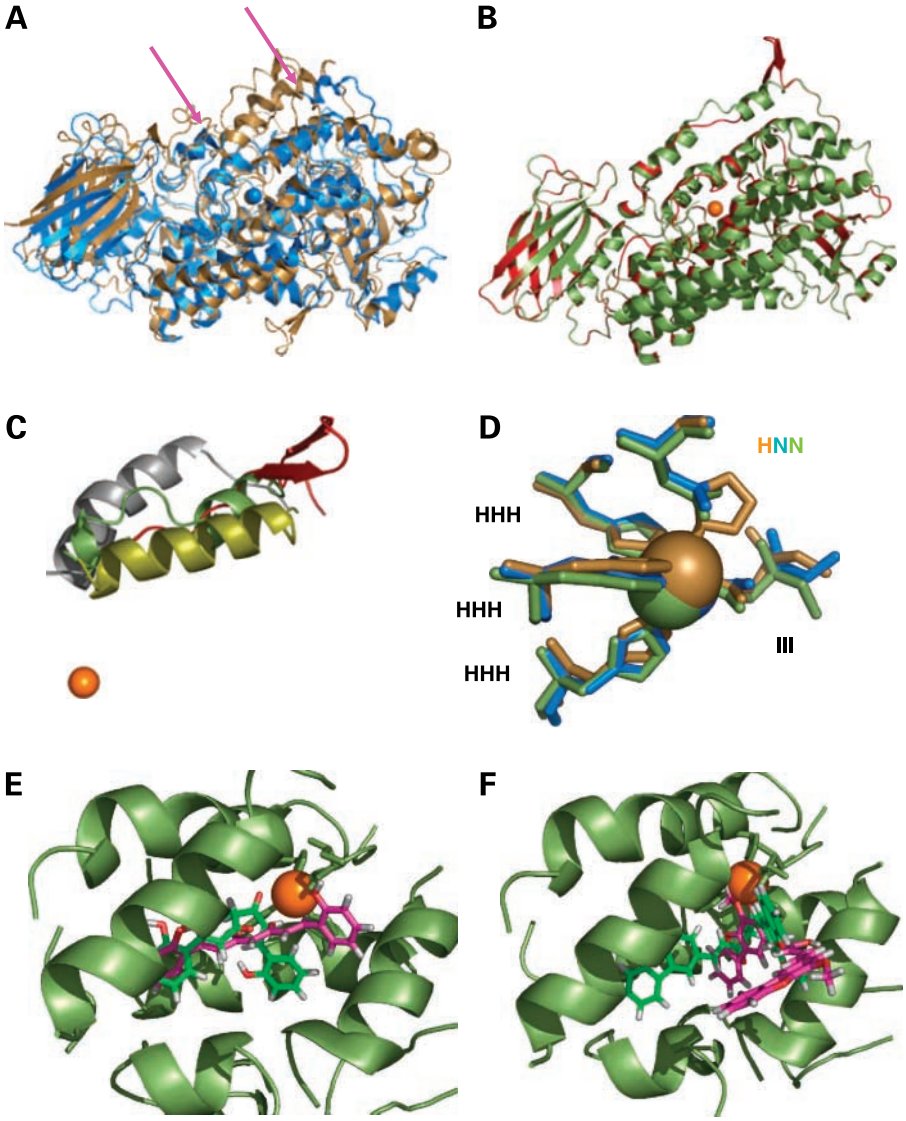

Figure 1. Ribbon models of soybean lipoxygenase (*light brown*), rabbit (*light blue*), the automatic model of human P-12-LOX from Swiss-Model Repository (*red*), corrected and verified model (*light green*), iron cofactor (*orange sphere*). **A,** alignment of soybean lipoxygenase (1JNQ) over rabbit 15-LOX (1LOX). **B,** alignment of the automatic model over corrected model of human P-12-LOX, most differences in loop 175 to 195, that according to theoretical predictions should be helical in nature. **C,** alignment of the fragments 174 to 198 for the automatic model (*red*), two calculated models (*silver* and *yellow-green*), and manually verified model shown (*light green*). **D,** alignment of active site P-12-LOX model over rabbit 1LOX and soybean 1JNQ. **E,** E22C docked into the active site of h-P-12-LOX: keto form carbons (*green*), enol form carbons (*magenta*). **F,** E26C docked into the active site of h-P-12-LOX, colors as in **E**.

models (see Fig. 1C, *silver* and *yellow/green models*). All considered models differ substantially in the relative orientation and structure of the 175 to 195 fragment while showing high correlation in the molecule core. This upper fragment above the active site shows greater flexibility than the core of the molecule in soy and rabbit enzyme; hence, it is possible that it might be a common feature in other lipoxygenases as well. The docking procedure that was used to test binding of curcuminoids allows flexibility for the protein, and the defined receptor site does not encompass the above fragment. Therefore, we feel that our carefully examined, predicted molecule of P-12-LOX (Fig. 1B, *light green*) provides a sufficiently accurate approximation to serve well the purpose of this research.

Molecular Modeling of P-12-LOX Inhibition

Commercial curcumin isolated from the rhizome of the plant *Curcuma longa* contains three major curcuminoids: ~77% curcumin, 17% demethoxycurcumin, and 3% bisdemethoxycurcumin (49). In the literature, these chemicals are referred as natural curcuminoids (50), as opposed to synthetic curcuminoids, which are related to curcumin but undergo significant chemical modification (50, 51). Because natural curcuminoids show a consistently lower activity than curcumin in many different assays, our search for better inhibitors of P-12-LOX was limited to synthetic curcuminoids (52–54).

Initially, a three-dimensional database of known inhibitors of various lipoxygenases was created. Low-energy conformers of these ligand candidates were generated with Omega (OpenEye Scientific Software, Inc., Santa Fee, NM). From the total of 106 compounds, 80 where docked into the cavity containing the active site of P-12-LOX. The results from docking were scored independently by SLIDE and DrugScore. The ligand candidates were ranked based on their consensus score computed as the sum of their normalized DrugScores and SLIDE scores. It has been

Table 1. Structure and properties of compounds tested for P-12-LOX inhibition

Name	Structure	Docking rank	*A*	*B*	Log *P* keto*/enol†	*C*	IC_{50} (μmol/L)
Curcumin	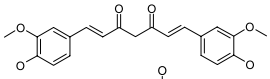	19*	61	1.7	2.3	0	66.0 ± 4.6
NDGA	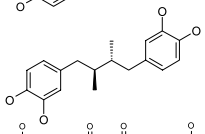	15	30	0.8	3.5	0	1.7 ± 5.0
E22C	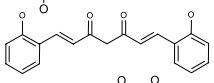	22*	266	0.2	3.6	0	12.3 ± 2.6
E26C	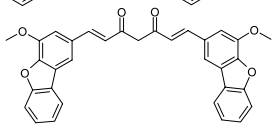	1*	25	3.3	6.6	2‡,§	17.0 ± 1.0
E16C	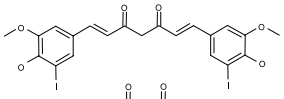	ND	ND	ND	4.8	2‡	>100
E17C	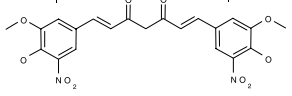	23*	17	2.9	2.5	1‖	>100
E19C	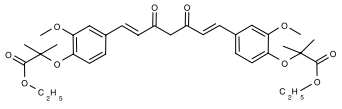	70*	4	8.7	6.8	2‡,§	>100
E25C	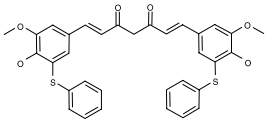	2†	9	6.7	7.3	2‡,§	>100
E27C	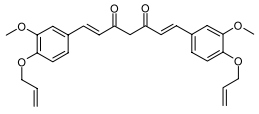	4*	8	2.8	4.2	0	>100
E35C	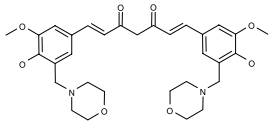	ND	ND	ND	1.9	1‡	>100
E57C	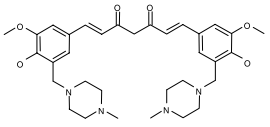	ND	ND	ND	2.0	1‡	>100

NOTE: *A*, number of docked orientations/molecule. *B*, distance from geometric center of the molecule to the center of the binding site (shortest distance listed in Å). *C*, number of Lipinsky rule violations.
Abbreviation: ND, not docked.

*Keto form: 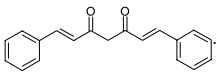

†Enol form: 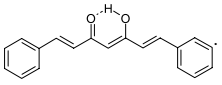

‡Molecular weight >500.
§Log *P* > 5.
‖Number of O and N atoms >10.

Table 2. Number of docked orientations and center distance for the compounds tested for P-12-LOX inhibition

Name	Docking Rank	No. docked orientations	Center distance (Å)	True inhibitor
Curcumin	19*	61	1.7	Yes
NDGA	15*	30	0.8	Yes
E22C	22*	266	0.2	Yes
E26C	1*	25	3.3	Yes
E16C	—	0	—	No
E17C	23*	17	2.9	No
E19C	70*	4	8.7	No
E25C	2†	6	6.8	No
E27C	4*	8	2.8	No
E35C	—	0	—	No
E57C	—	0	—	No

NOTE: Only the higher-ranking form (keto or enol) is listed for each compound.
*Keto.
†Enol.

shown repeatedly that consensus scoring improves hit rates in computational screening (55–57). To test our theoretical predictions, we determined the inhibitory activity of all curcuminoids using recombinant human P-12-LOX. The ranks of the experimentally tested ligand candidates together with their log *P*s calculated with Interactive logP calculator are listed in Table 1.[5]

Given the known limitations of existing scoring functions in correctly predicting binding affinities, additional features were also considered and computed to help discriminate true positive hits from false positives. One of these features is the number of docked orientations per molecule (Table 2), which in case of docking with SLIDE is proportional to the number of possible matches between different ligand interaction point triplets and template triangles. The more similar the shape and chemistry of the ligand to the template describing the binding site, the more docked orientations can result. Another feature describing how well the docked ligand is buried in the binding site is the distance between the geometric center of the docked ligand and the geometric center of the template (Table 2). The shorter this distance, the smaller the part of the docked ligand only partially buried in the binding site or completely exposed. True positive inhibitors were found to dock with a larger number of orientations and tended to be well buried and closer to the center of the binding site, than false positives. Such relationships between geometric and chemical features of the modeled protein-ligand complex, even if not generally valid across various systems are valuable for identifying additional new inhibitors for P-12-LOX. The top scoring binding orientations of the compounds that we confirmed to have P-12-LOX inhibitory activity exhibit some common binding motifs. One of the aromatic rings is stacked invariantly between the plane of the side chain carboxylic acid of Glu^{355} and the side chain of Ile^{592}, with two other aromatic rings (Phe^{351} and Phe^{413}) positioned in a perpendicular way around it. These residues form an ideal pocket for binding an aromatic ring. The other aromatic ring docked next to His^{364} into the hydrophobic pocket lined by Leu^{360}, Ile^{398}, Leu^{406}, Ala^{402} in the case of NDGA, or, alternatively, in the pocket defined by Trp^{143}, Leu^{407}, Leu^{360}, Leu^{365} in the case of larger ligands. Thus, two hydrophobic groups, at least one of them aromatic, connected by a flexible linker seems to be necessary for binding strongly enough to inhibit the enzyme. Some of the molecules we tested have hydrophobic groups that are too bulky; thus, they were docked with only one half buried into the binding site (E19C and E25C) or could not be docked at all (E35C and E57C). These compounds turned out not to have inhibitory activity in experimental testing.

Enzyme Characterization

Histidine-tagged human P-12-LOX with a 6-His tag on the NH_2 terminus yielded ~95% pure protein in single step purification using 6xHis affinity column as determined by PAGE gel densitometry (Fig. 2). A Western blot with anti-6-His antibody showed a band exactly in the same position as standard P-12-LOX. P-12-LOX was produced and purified in ~20 mg/L of cell culture. In the absence of the h-P-12-LOX antibody, protein identity was confirmed by mass spectroscopy (Table 3; Fig. 3). Collision-induced dissociation spectra were manually verified by comparing against an *in silico* tryptic digest of P-12-LOX sequence using the MS-Digest and MS-Product provisions of Protein Prospector.[4] At dominant band, only P-12-LOX peptides were found confirming the identity of this protein.

The enzyme was found to be active, showing K_m = 15.6 μmol/L, and V_{max} = 1.5 μmol/L/min. The measured values for P-12-LOX were very similar to values found by others for the same enzyme (K_m ~ 10 μmol/L, V_{max} ~ 2 μmol/L/min; refs. 44, 58). The maximum activity was observed at pH 8 (Fig. 4), and this is also consistent with

[5] http://www.molinspiration.com/cgi-bin/properties

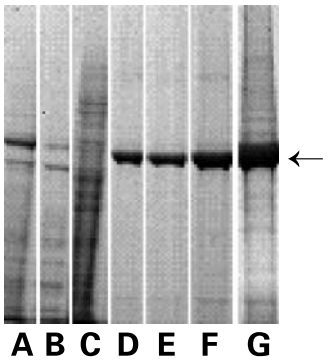

Figure 2. Coomassie blue stain of (**A**) cell lysate, (**B**) flow thought from column, (**C**) wash, (**D**) elutant 1 times, **E** 1.5 times, **F** 2.5 times, **G** 15 times higher than (**D**). Arrow indicates P-12-LOX. Photograph was electronically enhanced to show potential contaminants (visible on **F** and **G** only). Purity of P-12-LOX was determined as +95%.

previous reports (44, 58). The iron content was measured by atomic absorption spectroscopy and was determined as 0.45 ± 0.10 mol of iron per 1 mol of enzyme. A second independent measurement was done by inductively coupled plasma optical emission spectroscopy at <9 ppm, which translates into a molecular ratio of 0.7. This method required a very large amount of protein for analysis (20 mg), and for this reason, only one measurement was done. Theoretically, the stoichiometric ratio is expected to be 1:1, but in practice, the iron cofactor can be easily washed out; therefore, its content in a protein sample is usually lower. This is a common finding for lipoxygenases: Matsuda et al. cited 0.7 for porcine leukocyte 12-LOX (59), and Segraves and Holman have quoted 0.35 for human P-12-LOX (60).

Synthetic Curcuminoids Inhibit Human P-12-LOX

As shown in Table 1, P-12-LOX was inhibited by curcumin, NDGA, E22C, and E26C. NDGA is a known lipoxygenases inhibitor, and its IC_{50} reported by Amagata et al. is identical with the value determined by us (44). Curcumin is the known inhibitor of other lipoxygenase types, and it is no surprise that we found it inhibits P-12-LOX as well (23, 61). In general, we have found that computational predictions (e.g., high rank of docked ligands, low log *P*s) agreed with the ability of the compounds to inhibit P-12-LOX.

Synthetic Curcuminoids Inhibit Sprout Formation

The significance of cancer-related neovascularization has been characterized over the past two decades (62). Angiogenesis is a prerequisite of tumor growth and is the target of drug development in many preclinical and clinical trials. Angiogenesis is a multistep progression in physiologic and pathologic processes. It involves endothelial cell sprouting from the parent vessel followed by migration, proliferation, tube formation, and connecting to other vessels (63). Several *in vitro* models have attempted to recreate this complex sequence of events with varying degrees of success. Angiogenic sprouting and capillary lumen formation in fibrin gel is one of the commonly accepted models of angiogenesis *in vitro* and provides a powerful tool for analysis of this complex phenomenon.

When HUVEC aggregates were treated (Fig. 5) with synthetic E22C and E26C curcuminoids with NDGA as a control, a significant reduction in sprout length and sprout number was observed. Sprouting ability of endothelial cells is related to stimulation by vascular endothelial growth factor. Nie et al. showed that endothelial cells synthesize various eicosanoids, including the 12-LOX product 12(*S*)-HETE, and that endogenous 12-LOX is involved in endothelial cell angiogenic responses. They have showed that 12-LOX inhibitors reduced endothelial cell proliferation by down-regulation of vascular endothelial growth factor (64). That phenomenon could explain reduction in number of sprouts formed in our experiments. It has been reported by Rondeau et al. that NDGA down-regulates urokinase plasminogen activator mRNA level and urokinase plasminogen activator biosynthesis via protein kinase C and/or lipoxygenases pathways also (65). Urokinase plays a major role in extracellular proteolytic events associated with angiogenesis (66), and reduced urokinase

Table 3. Sequence of peptides extracted from dominant band of PAGE gel

Access no.	Protein names	Theoretical mass	Observed mass	Peptide	Sequence
P18054	Arachidonate 12-LOX, 12(*S*)-type (12-LOX; P-12-LOX)	1,770.90	1,771.02	98-113	WVQGEDILSLPEGTAR
		1,364.65	1,364.24	114-125	LPGDNALDmFQK
		1,155.63	1,155.48	145-155	EGLPLTIAADR
		1,207.64	1,207.44	169-177	RLDFEWTLK
		919.49	919.44	178-187	AGALEmALK
		1,800.94	1,801.18	249-265	LVLPSGmEELQAQLEK
		1,784.94	1,784.63	249-265	LVLPSGMEELQAQLEK
		1,043.48	1,043.18	394-401	YTmEINTR
		1,293.66	1,293.28	404-415	TQLISDGGIFDK
		1,636.91	1,636.82	449-465	GLLGLPGALYAHDALR
		1,523.80	1,523.30	473-484	YVEGIVHLFYQR
		847.47	847.84	621-627	AVLNQFR

Abbreviation: m, oxidized methionine.

Figure 3. Sequence of human P-12-LOX. Amino acids shown in bold were detected by mass spectroscopy as indicated in Table 3. *Arrows,* potential trypsin cleavage site.

```
                        10 |       20 |       30 |       40 |       50 |       60 |
h-P-12-LOX      GRYRIRVATG AWLFSGSYNR VQLWLVGTRG EAELELQLRP ARGEEEEFDH DVAEDLGLLQ  60
6His h-P-12-LOX ---------- ---------- ---------- ---------- ---------- ----------
                 ↑ ↑ ↑              ↑          ↑          ↑  ↑
h-P-12-LOX      FVRLRKHHWL VDDAWFCDRI TVQGPGACAE VAFPCYRWVQ GEDILSLPEG TARLPGDNAL 120
6His h-P-12-LOX ---------- ---------- ---------- -------WVQ GEDILSLPEG TARLPGDNAL
                  ↑ ↑↑              ↑                     ↑                    ↑
h-P-12-LOX      DMFQKHREKE LKDRQQIYCW ATWKEGLPLT IAADRKDDLP PNMRFHEEKR LDFEWTLKAG 180
6His h-P-12-LOX DMFQK----- ---------- ----EGLPLT IAADR----- ---------R LDFEWTLKAG
                    ↑ ↑ ↑   ↑ ↑        ↑          ↑↑          ↑   ↑↑          ↑
h-P-12-LOX      ALEMALKRVY TLLSSWNCLE DFDQIFWGQK SALAEKVRQC WQDDELFSYQ FLNGANPMLL 240
6His h-P-12-LOX ALEMALK--- ---------- ---------- ----------  ---------- ----------
                                                 ↑      ↑ ↑
h-P-12-LOX      RRSTSLPSRL VLPSGMEELQ AQLEKELQNG SLFEADFILL DGIPANVIRG EKQYLAAPLV 300
6His h-P-12-LOX ---------L VLPSGMEELQ AQLEK----- ---------- ---------- ----------
                ↑↑      ↑           ↑                                ↑    ↑
h-P-12-LOX      MLKMEPNGKL QPMVIQIQPP SPSSPTPTLF LPSDPPLAWL LAKSWVRNSD FQLHEIQYHL 360
6His h-P-12-LOX ---------- ---------- ---------- ---------- ---------- ----------
                  ↑     ↑                                   ↑    ↑
h-P-12-LOX      LNTHLVAEVI AVATMRCLPG LHPIFKFLIP HIRYTMEINT RARTQLISDG GIFDKAVSTG 420
6His LOX        ---------- ---------- ---------- ---YTMEINT R--TQLISDG GIFDK-----
                           ↑          ↑          ↑          ↑↑          ↑
h-P-12-LOX      GGGHVQLLRR AAAQLTYCSL CPPDDLADRG LLGLPGALYA HDALRLWEII ARYVEGIVHL 480
6His h-P-12-LOX ---------- ---------- ---------G LLGLPGALYA HDALR----- --YVEGIVHL
                         ↑↑                    ↑                    ↑     ↑
h-P-12-LOX      FYQRDDIVKG DPELQAWCRE ITEVGLCQAQ DRGFPVSFQS QSQLCHFLTM CVFTCTAQHA 540
6His h-P-12-LOX FYQR------ ---------- ---------- ---------- ---------- ----------
                   ↑    ↑          ↑                    ↑
h-P-12-LOX      AINQGQLDWY AWVPNAPCTM RMPPPTTKED VTMATVMGSL PDVRQACLQM AISWHLSRRQ 600
6His h-P-12-LOX ---------- ---------- ---------- ---------- ---------- ----------
                                     ↑     ↑               ↑                   ↑↑
h-P-12-LOX      PDMVPLGHHK EKYFSGPKPK AVLNQFRTDL EKLEKEITAR NEQLDWPYEY LKPSCIENSV 660
6His h-P-12-LOX ---------- ---------- AVLNQFR--- ---------- ---------- ----------
                         ↑  ↑    ↑ ↑      ↑     ↑  ↑    ↑           ↑
h-P-12-LOX      TI                                                              662
6His h-P-12-LOX --
```

plasminogen activator activity of HUVECs by lipoxygenase inhibitors would reduce length in sprout formation assay, which to propagate must hydrolyze fibrin gel.

Results are presented in Fig. 6 as a percentage relative to untreated control sprouts. These results are statistically significant starting at concentrations higher than IC_{50} for all inhibitors tested. The ability of curcumin to affect gene transcription and to induce apoptosis is likely to be of particular significance in cancer chemoprevention and chemotherapy in patients. However, curcumin's low systemic bioavailability following oral administration may be a limiting factor to assure sufficient concentrations for pharmacologic effect in certain tissues. Furthermore, curcumin and natural curcuminoids possess anti-inflammatory and anticancer properties following oral or topical administration. Separately from antioxidant properties of these compounds, the mechanisms of action include inhibition of enzymes, such as lipoxygenases, cyclooxygenases, inducible nitric oxide synthase, and xanthine dehydrogenase/oxidase (67). Curcumin is also a potent inhibitor of the protein kinase C, epidermal growth factor receptor tyrosine kinase, and IκB kinase. Additionally, curcumin inhibits the activation of NFκB and the expression of c-*jun*, c-*fos*, and c-*myc* (68, 69). NDGA is a phenolic compound isolated from the creosote bush *Larrea divaricatta* that has been reported to inhibit lipoxygenases and has anti-cancer activities as well. These are attributed to the

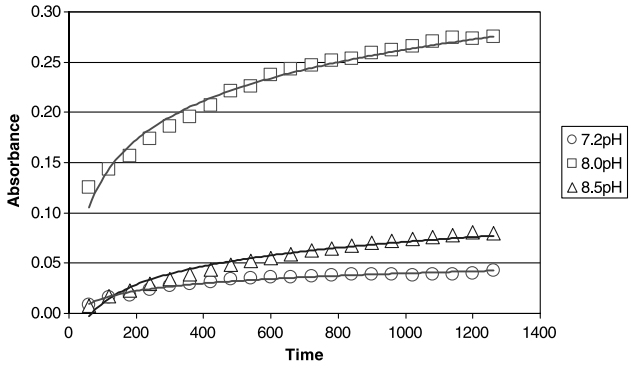

Figure 4. Increase of concentration of 12(*S*)-HETE as a function of time and pH measured as an increase of absorbance at 234 nm. Similar dependence was observed when different P-12-LOX inhibitors where used.

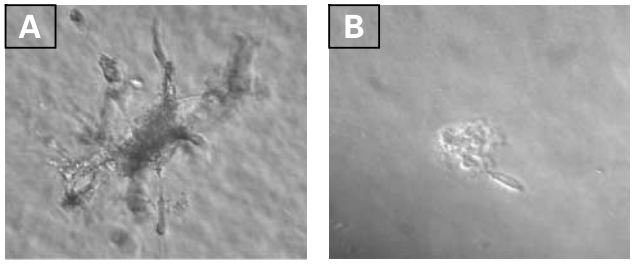

Figure 5. Sprout formation of human endothelial cells: (**A**) control, treaded with 30 μmol/L E26C.

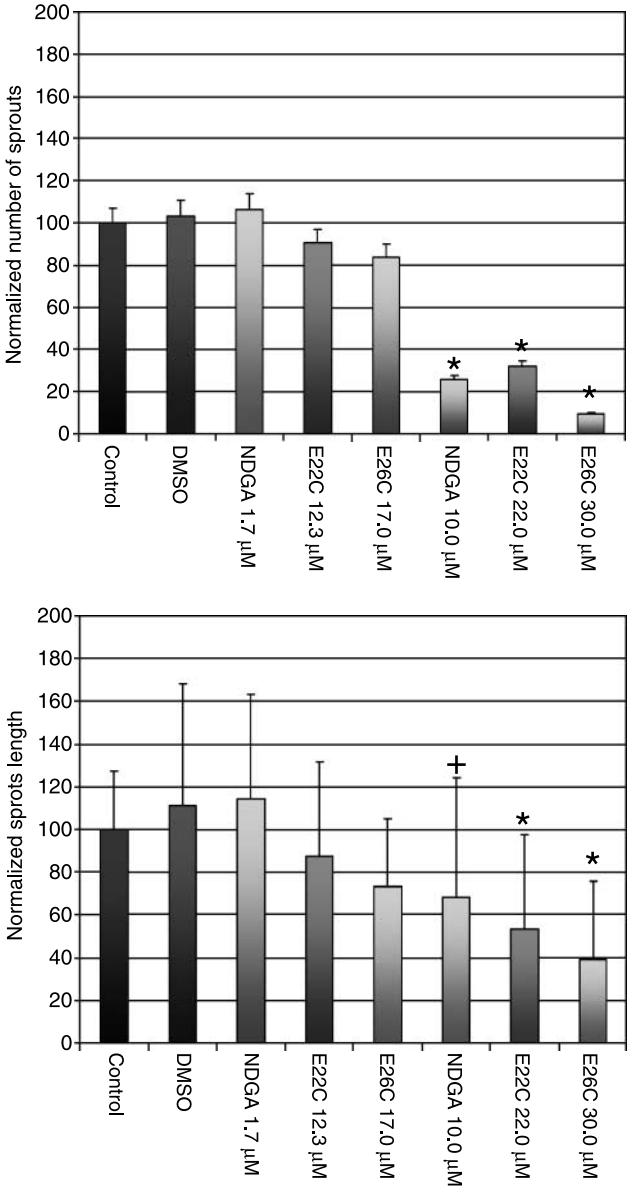

Figure 6. Normalized number and length of human endothelial cells treated with different P-12-LOX inhibitors. *, statistically significant differences versus control and DMSO; +, statistically significant differences versus DMSO.

ability of NDGA to directly inhibit the function of important in carcinogenesis receptors: tyrosine kinases, insulin-like growth factor, and *c-erbB2/HER-2/neu* receptors (70).

Inhibition of any of these proteins could be of therapeutic significance. What is important in our experiments is the limited inhibition of sprout formation at concentrations ~IC_{50} for human P-12-LOX of inhibitors tested. Even under this condition (IC_{50}), a substantial amount of 12-HETE can be produced by lipoxygenase, providing a stimulus for angiogenic sprouting of endothelial cells. Increasing the concentrations of lipoxygenase inhibitors above IC_{50} greatly reduces sprout formation for all inhibitors tested. It should be noted that this phenomenon was observed in different concentrations. For example, NDGA inhibited sprout formation in a concentration of 10 μmol/L (>IC_{50}), whereas E26C at a concentration of 17 μmol/L (IC_{50}) did not. This universal event for all tested lipoxygenase inhibitors suggests that inhibition of sprout formation was most likely due to the inhibition of human P-12-LOX but not other cancer-related pathways.

Although this is still not an exhaustive demonstration of a specific inhibition of P-12-LOX by curcuminoids, we conclude that protein structure-based ligand selection supported by theoretical log *P* determination and structural analysis of ligands binding to human P-12-LOX is in a good agreement with *in vitro* effects of lipoxygenase inhibition by different curcuminoids. Furthermore, successful selection of two novel lipoxygenase inhibitors by combination of computational and biochemical methods provides template for future search of novel P-12-LOX inhibitors from very large database of three-dimensional structures.

Acknowledgments

We thank Dr. R. Hart (President of American Diagnostica, Inc., Stamford, CT) for his support and the chemicals used in this study, Dr. Gerhard Klebe (University of Marburg, Germany) for providing DrugScore, and OpenEye Scientific Software for providing Omega for our use.

References

1. Pidgeon GP, Kandouz M, Meram A, Honn KV. Mechanisms controlling cell cycle arrest and induction of apoptosis after 12-lipoxygenase inhibition in prostate cancer cells. Cancer Res 2002;62:2721 – 7.

2. Chan JM, Gann PH, Giovannucci EL. Role of diet in prostate cancer development and progression. J Clin Oncol 2005;23:8152 – 60.

3. Funk CD. The molecular biology of mammalian lipoxygenases and the quest for eicosanoid functions using lipoxygenase-deficient mice. Biochim Biophys Acta 1996;1304:65 – 84.

4. Funk CD, Chen XS, Johnson EN, Zhao L. Lipoxygenase genes and their targeted disruption. Prostaglandins Other Lipid Mediat 2002;68 – 9: 303 – 12.

5. Timar J, Raso E, Dome B, et al. Expression, subcellular localization and putative function of platelet-type 12-lipoxygenase in human prostate cancer cell lines of different metastatic potential. Int J Cancer 2000;87: 37 – 43.

6. Gao X, Grignon DJ, Chbihi T, et al. Elevated 12-lipoxygenase mRNA expression correlates with advanced stage and poor differentiation of human prostate cancer. Urology 1995;46:227 – 37.

7. Nie D, Nemeth J, Qiao Y, et al. Increased metastatic potential in human prostate carcinoma cells by overexpression of arachidonate 12-lipoxygenase. Clin Exp Metastasis 2003;20:657 – 63.

8. Timar J, Tovari J, Raso E, Meszaros L, Bereczky B, Lapis K. Platelet-mimicry of cancer cells: epiphenomenon with clinical significance. Oncology 2005;69:185 – 201.

9. Eling TE, Glasgow WC. Cellular proliferation and lipid metabolism: importance of lipoxygenases in modulating epidermal growth factor-dependent mitogenesis. Cancer Metastasis Rev 1994;13:397 – 410.

10. Honn KV, Timar J, Rozhin J, et al. A lipoxygenase metabolite, 12-(*S*)-HETE, stimulates protein kinase C-mediated release of cathepsin B from malignant cells. Exp Cell Res 1994;214:120 – 30.

11. Tang DG, Renaud C, Stojakovic S, Diglio CA, Porter A, Honn KV. 12(*S*)-HETE is a mitogenic factor for microvascular endothelial cells: its potential role in angiogenesis. Biochem Biophys Res Commun 1995;211: 462 – 8.

12. Nie D, Hillman GG, Geddes T, et al. Platelet-type 12-lipoxygenase in a human prostate carcinoma stimulates angiogenesis and tumor growth. Cancer Res 1998;58:4047 – 51.

13. Tang DG, Diglio CA, Honn KV. Activation of microvascular endothelium by eicosanoid 12(*S*)-hydroxyeicosatetraenoic acid leads to enhanced tumor cell adhesion via up-regulation of surface expression of alpha v beta 3 integrin: a posttranscriptional, protein kinase C- and cytoskeleton-dependent process. Cancer Res 1994;54:1119 – 29.

14. Honn KV, Grossi IM, Diglio CA, Wojtukiewicz M, Taylor JD. Enhanced tumor cell adhesion to the subendothelial matrix resulting from 12(*S*)-HETE-induced endothelial cell retraction. FASEB J 1989;3:2285 – 93.

15. Silletti S, Timar J, Honn KV, Raz A. Regulation of tumor cell motility by 12(*S*)-HETE. Adv Exp Med Biol 1997;400B:683 – 92.

16. Liu B, Maher RJ, De Jonckheere JP, et al. 12(*S*)-HETE increases the motility of prostate tumor cells through selective activation of PKC alpha. Adv Exp Med Biol 1997;400B:707 – 18.

17. McCabe NP, Selman SH, Jankun J. Vascular endothelial growth factor production in human prostate cancer cells is stimulated by overexpression of platelet 12-lipoxygenase. The Prostate 2006;66: 779 – 87.

18. Connolly JM, Rose DP. Enhanced angiogenesis and growth of 12-lipoxygenase gene-transfected MCF-7 human breast cancer cells in athymic nude mice. Cancer Lett 1998;132:107 – 12.

19. Miocinovic R, McCabe NP, Keck RW, Jankun J, Hampton JA, Selman SH. *In vivo* and *in vitro* effect of baicalein on human prostate cancer cells. Int J Oncol 2005;26:241 – 6.

20. Sinha R, Anderson DE, McDonald SS, Greenwald P. Cancer risk and diet in India. J Postgrad Med 2003;49:222 – 8.

21. Chainani-Wu N. Safety and anti-inflammatory activity of curcumin: a component of tumeric (*Curcuma longa*). J Altern Complement Med 2003; 9:161 – 8.

22. Iqbal M, Sharma SD, Okazaki Y, Fujisawa M, Okada S. Dietary supplementation of curcumin enhances antioxidant and phase II metabolizing enzymes in ddY male mice: possible role in protection against chemical carcinogenesis and toxicity. Pharmacol Toxicol 2003;92:33 – 8.

23. Cuendet M, Pezzuto JM. The role of cyclooxygenase and lipoxygenase in cancer chemoprevention. Drug Metabol Drug Interact 2000;17:109 – 57.

24. Hong J, Bose M, Ju J, et al. Modulation of arachidonic acid metabolism by curcumin and related {beta}-diketone derivatives: effects on cytosolic phospholipase A2, cyclooxygenases, and 5-lipoxygenase. Carcinogenesis 2004;25:1671 – 9.

25. Aggarwal BB, Kumar A, Bharti AC. Anticancer potential of curcumin: preclinical and clinical studies. Anticancer Res 2003;23:363 – 98.

26. Skrzypczak-Jankun E, McCabe NP, Selman SH, Jankun J. Curcumin inhibits lipoxygenase by binding to its central cavity: theoretical and X-ray evidence. Int J Mol Med 2000;6:521 – 6.

27. Schwede T, Kopp J, Guex N, Peitsch MC. SWISS-MODEL: an automated protein homology-modeling server. Nucleic Acids Res 2003; 31:3381 – 5.

28. Schwede T, Diemand A, Guex N, Peitsch MC. Protein structure computing in the genomic era. Res Microbiol 2000;151:107 – 12.

29. Gillmor SA, Villasenor A, Fletterick R, Sigal E, Browner MF. The structure of mammalian 15-lipoxygenase reveals similarity to the lipases and the determinants of substrate specificity. Nat Struct Biol 1997;4: 1003 – 9.

30. Boyington JC, Gaffney BJ, Amzel LM. The three-dimensional structure of soybean lipoxygenase-1: an arachidonic acid 15-lipoxygenase. Adv Exp Med Biol 1997;400A:133 – 8.

31. Skrzypczak-Jankun E, Borbulevych OY, Jankun J. Soybean lipoxygenase-3 in complex with 4-nitrocatechol. Acta Crystallogr D Biol Crystallogr 2004;60:613 – 5.

32. Skrzypczak-Jankun E, Zhou K, Jankun J. Inhibition of lipoxygenase by (-)-epigallocatechin gallate: X-ray analysis at 2.1 A reveals degradation of EGCG and shows soybean LOX-3 complex with EGC instead. Int J Mol Med 2003;12:415 – 20.

33. Skrzypczak-Jankun E, Bross RA, Carroll RT, Dunham WR, Funk MO, Jr. Three-dimensional structure of a purple lipoxygenase. J Am Chem Soc 2001;123:10814 – 20.

34. Tanaka N, Haga A, Uemura H, et al. Inhibition mechanism of cytokine activity of human autocrine motility factor examined by crystal structure analyses and site-directed mutagenesis studies. J Mol Biol 2002;318: 985 – 97.

35. Sack JS. CHAIN: a crystallographic modeling program. J Mol Graph 1988;6:224 – 5.

36. Fiser A, Feig M, Brooks CL III, Sali A. Evolution and physics in comparative protein structure modeling. Acc Chem Res 2002;35:413 – 21.

37. Fiser A, Sali A. ModLoop: automated modeling of loops in protein structures. Bioinformatics 2003;19:2500 – 1.

38. Brooks BR, Bruccoleri RE, Olafson BD, States DJ, Swaminathan S, Karplus M. CHARMM: a program for macromolecular energy, minimization, and dynamics calculations. Journal Computaional Chemistry 1983;4: 187 – 217.

39. Feig m, Karanicolas J, Brooks CL III. MMTSB tool set: enhanced sampling and multiscale modeling methods for applications in structural biology. J Mol Graph Model 2004;22:377 – 95.

40. Schnecke V, Kuhn LA. Virtual screening with solvation and ligand-induced complementarity. Perspectives in Drug Discovery and Design 2000;20:171 – 90.

41. Zavodszky MI, Sanschagrin PC, Korde RS, Kuhn LA. Distilling the essential features of a protein surface for improving protein-ligand docking, scoring, and virtual screening. J Comput Aided Mol Des 2002; 16:883 – 902.

42. Gohlke H, Hendlich M, Klebe G. Knowledge-based scoring function to predict protein-ligand interactions. J Mol Biol 2000;295:337 – 56.

43. Guex N, Peitsch MC. SWISS-MODEL and the Swiss-PdbViewer: an environment for comparative protein modeling. Electrophoresis 1997;18: 2714 – 23.

44. Amagata T, Whitman S, Johnson TA, et al. Exploring sponge-derived terpenoids for their potency and selectivity against 12-human, 15-human, and 15-soybean lipoxygenases. J Nat Prod 2003;66:230 – 5.

45. Basrur V, Yang F, Kushimoto T, et al. Proteomic analysis of early melanosomes: identification of novel melanosomal proteins. J Proteome Res 2003;2:69 – 79.

46. Jankun J, Specht Z, Szkudlarek M, et al. Plasminogen activator inhibitor-1 is locked in active conformation and polymerizes upon binding ligands neutralizing its activity. Int J Mol Med 2006;17:437 – 47.

47. Pepper MS, Montesano R, Vassalli JD, Orci L. Chondrocytes inhibit endothelial sprout formation *in vitro*: evidence for involvement of a transforming growth factor-beta. J Cell Physiol 1991;146:170 – 9.

48. Altschul SF, Madden TL, Schaffer AA, et al. Gapped BLAST and PSI-BLAST: a new generation of protein database search programs. Nucleic Acids Res 1997;25:3389 – 402.

49. Huang MT, Newmark HL, Frenkel K. Inhibitory effects of curcumin on tumorigenesis in mice. J Cell Biochem Suppl 1997;27:26 – 34.

50. Limtrakul P, Anuchapreeda S, Buddhasukh D. Modulation of human multidrug-resistance MDR-1 gene by natural curcuminoids. BMC Cancer 2004;4:13.

51. Leyon PV, Kuttan G. Studies on the role of some synthetic curcuminoid derivatives in the inhibition of tumour specific angiogenesis. J Exp Clin Cancer Res 2003;22:77 – 83.

52. Ramsewak RS, DeWitt DL, Nair MG. Cytotoxicity, antioxidant and anti-inflammatory activities of curcumins I-III from *Curcuma longa*. Phytomedicine 2000;7:303 – 8.

53. Kang HM, Son KH, Yang DC, et al. Inhibitory activity of diarylheptanoids on farnesyl protein transferase. Nat Prod Res 2004;18:295 – 9.

54. Chearwae W, Anuchapreeda S, Nandigama K, Ambudkar SV, Limtrakul P. Biochemical mechanism of modulation of human P-glycoprotein (ABCB1) by curcumin I, II, and III purified from Turmeric powder. Biochem Pharmacol 2004;68:2043 – 52.

55. Clark RD, Strizhev A, Leonard JM, Blake JF, Matthew JB. Consensus scoring for ligand/protein interactions. J Mol Graph Model 2002;20:281 – 95.

56. Mozziconacci JC, Arnoult E, Bernard P, Do QT, Marot C, Morin-Allory L. Optimization and validation of a docking-scoring protocol; application to virtual screening for COX-2 inhibitors. J Med Chem 2005; 48:1055 – 68.

57. Cotesta S, Giordanetto F, Trosset JY, et al. Virtual screening to enrich a compound collection with CDK2 inhibitors using docking, scoring, and composite scoring models. Proteins 2005;60:629 – 43.

58. Chen XS, Brash AR, Funk CD. Purification and characterization of

recombinant histidine-tagged human platelet 12-lipoxygenase expressed in a baculovirus/insect cell system. Eur J Biochem 1993;214:845 – 52.

59. Matsuda S, Suzuki H, Yoshimoto T, Yamamoto S, Miyatake A. Analysis of non-heme iron in arachidonate 12-lipoxygenase of porcine leukocytes. Biochim Biophys Acta 1991;1084:202 – 4.

60. Segraves EN, Holman TR. Kinetic investigations of the rate-limiting step in human 12- and 15-lipoxygenase. Biochemistry 2003;42:5236 – 43.

61. Hong J, Bose M, Ju J, et al. Modulation of arachidonic acid metabolism by curcumin and related beta-diketone derivatives: effects on cytosolic phospholipase A(2), cyclooxygenases and 5-lipoxygenase. Carcinogenesis 2004;25:1671 – 9.

62. Kerr DJ. Targeting angiogenesis in cancer: clinical development of bevacizumab. Nat Clin Pract Oncol 2004;1:39 – 43.

63. Nakatsu MN, Sainson RC, Aoto JN, et al. Angiogenic sprouting and capillary lumen formation modeled by human umbilical vein endothelial cells (HUVEC) in fibrin gels: the role of fibroblasts and Angiopoietin-1. Microvasc Res 2003;66:102 – 12.

64. Nie D, Tang K, Diglio C, Honn KV. Eicosanoid regulation of angiogenesis: role of endothelial arachidonate 12-lipoxygenase. Blood 2000;95:2304 – 11.

65. Rondeau E, Guidet B, Lacave R, et al. Nordihydroguaiaretic acid inhibits urokinase synthesis by phorbol myristate acetate-stimulated LLC-PK1 cells. Biochim Biophys Acta 1990;1055:165 – 72.

66. Heynekamp JJ, Hunsaker LA, Vander Jagt TA, Deck LM, Vander Jagt DL. Uncharged isocoumarin-based inhibitors of urokinase-type plasminogen activator. BMC Chem Biol 2006;6:1.

67. Shishodia S, Sethi G, Aggarwal BB. Curcumin: getting back to the roots. Ann N Y Acad Sci 2005;1056:206 – 17.

68. Sharma RA, Gescher AJ, Steward WP. Curcumin: the story so far. Eur J Cancer 2005;41:1955 – 68.

69. Lin JK, Lin-Shiau SY. Mechanisms of cancer chemoprevention by curcumin. Proc Natl Sci Counc Repub China B 2001;25:59 – 66.

70. Youngren JF, Gable K, Penaranda C, et al. Nordihydroguaiaretic acid (NDGA) inhibits the IGF-1 and c-erbB2/HER2/neu receptors and suppresses growth in breast cancer cells. Breast Cancer Res Treat 2005;94:37 – 46.